

Reading Course

Curved Surfaces & Thin Film Instabilities

Timothy Peters

January 2022

1 Introduction

This report is motivated by a reading course to explore thin film problems on different surfaces. Over the course of this report we derive the thin film equations for an arbitrary substrate using curvilinear coordinates, providing examples on how these break down to normal geometries such as a planar substrate and cylinder. We then proceed to explore papers published by Kondic & Lin which examine free surface instabilities which grow on an inverted substrate and a funnel. Finally we briefly mention some open challenges that stem from the rest of the report.

1.1 Background and Motivation

The problem of thin film flows is one that has been widely studied over the last 50 years. This thin film process is often seen in industrial settings such as the drying of paint or condensation on heat exchangers as well as natural processes such as the flow of a tear on an eye. In all these different settings, the film is thin and therefore mathematical models used to explain such systems are based on lubrication theory.

However, for many of the times the problem has been studied, analysis has been done for a flat substrate inclined at some angle. For example [Moriarty et al. \[1991\]](#) studied liquid falling on a wall under gravity as well as spreading under a jet of air, [King et al. \[1993\]](#) examined the problem under a pressure field which was coupled to the film height using airfoil theory identifying air blown waves, and [Myers \[1998\]](#) looked at different cases such as a contact lenses or drying paint. Of course, in many cases where thin films arise, the substrate itself is not flat so it important to be able to model such problems for different geometries.

One of the earliest examples of this is by [Wang \[1984\]](#). Later, the formulation was done for the modelling of coating flows on curved surfaces by [Schwartz and Weidner \[1995\]](#). However, this was for a one dimension curved surface. In the early 2000s however, this derivation was done independently by three groups [Myers et al. \[2002\]](#) [Roy et al. \[2002\]](#) and [Howell \[2003\]](#).

For these curved surface some groups have studied these in the context of quantifying the effect of curvature on the Ryaleigh Taylor instabilitiy. For example [Trinh et al. \[2014\]](#) examined the thin film in the context of the film on an underside of a

cylinder. The effect of the curvature of the substrate was studied whereby they found certain regimes in which the Rayleigh-Taylor instability was suppressed. This work was followed up on by [Balestra et al. \[2018\]](#) who performed a similar analysis for the underside of a sphere. Finally, work was presented by [Takagi and Huppert \[2010\]](#), examining the evolution of a thin film on top of a cylinder and sphere. However this only holds until the fluid splits in rivulets.

Studying the thin film instabilities that form on different substrates is also of interest. [Lin and Kondic \[2010\]](#) studied the instabilities from gravity driven flow on an inverted flat surface, whereby the thin film flow will start with a constant speed behind the wave front which will destabilise to produce different pulse trains. Later they studied the same problem [Lin et al. \[2012\]](#) but for the three-dimensional case examining the fingers which formed. Finally they examined the problem for a funnel ([Lin et al. \[2021\]](#)).

In our next section we discuss briefly our curvilinear coordinate system. We then proceed to derive the thin film equation for this coordinate system in section 2. In section 3 we discuss the work done by Kondic & Lin. In section 4 we briefly discuss the work done by Takagi & Huppert and some open challenges.

1.2 Coordinate system

Examining an arbitrary surface we parameterise using a curvilinear coordinate system. Given a substrate \mathcal{S} , we examine the lines of principal curvature and parameterise these using the variables s_1, s_2 , where there is a mapping from these coordinates to the standard cartesian coordinates

$$\begin{aligned} s_1 &= s_1(x, y, z), \\ s_2 &= s_2(x, y, z). \end{aligned}$$

Note: For a surface, the directions in which the curvature takes its maximum and minimum values in the normal plane, are call the principal directions. These are always orthogonal to each other.

We then can denote the position of any point on the substrate as $\mathbf{R} = \mathbf{R}(s_1, s_2)$. Our first two unit orthogonal vectors \mathbf{e}_1 and \mathbf{e}_2 we define to be tangential to s_1 and s_2 . We define our third to be the normal to \mathcal{S} and thus we can write a point in space as

$$\mathbf{r}(s_1, s_2, s_3) = \mathbf{R}(s_1, s_2) + s_3 \mathbf{n},$$

where s_3 gives the distance away from substrate along the normal to the substrate. We recover our substrate when $s_3 = 0$. This is shown in [Figure 1](#)

Following [Myers et al. \[2002\]](#) we use the fundamental forms of the surface,

$$\begin{aligned} E &= \mathbf{R}_1 \cdot \mathbf{R}_1, & F &= \mathbf{R}_1 \cdot \mathbf{R}_2, & G &= \mathbf{R}_2 \cdot \mathbf{R}_2, \\ L &= \mathbf{R}_{11} \cdot \mathbf{n}, & M &= \mathbf{R}_{12} \cdot \mathbf{n}, & N &= \mathbf{R}_{22} \cdot \mathbf{n} \end{aligned} \quad ,$$

where we define

$$\mathbf{R}_1 \equiv \frac{\partial \mathbf{R}}{\partial s_1}, \quad \mathbf{R}_2 \equiv \frac{\partial \mathbf{R}}{\partial s_2}$$

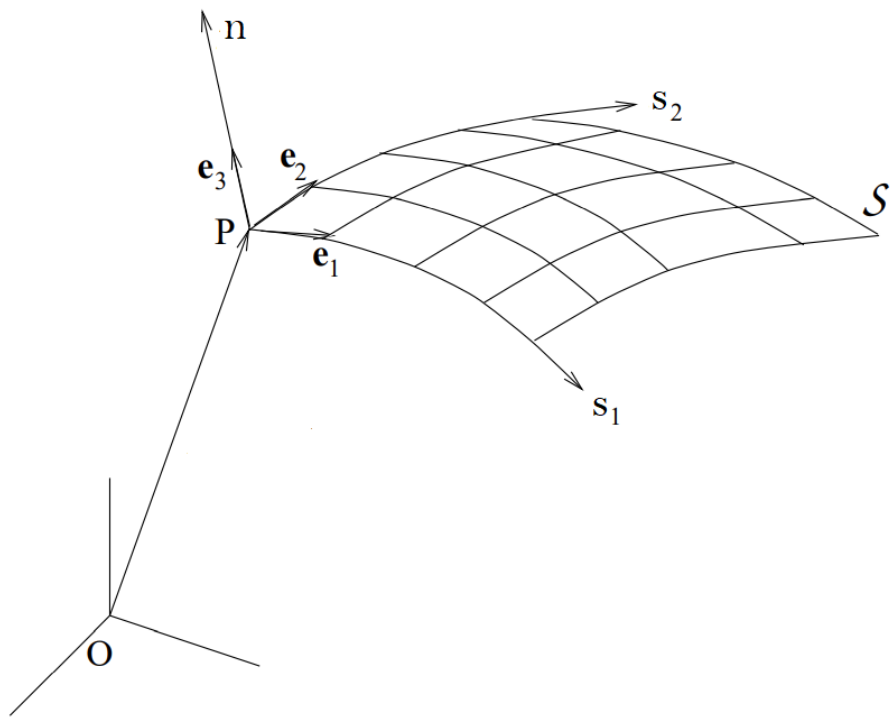


Figure 1: A representation of the parameterisation of our substrate by the lines of principal curvature s_1 and s_2 . Adapted from Roy et al. [2002].

and

$$\mathbf{n} = \frac{\mathbf{R}_1 \wedge \mathbf{R}_2}{|\mathbf{R}_1 \wedge \mathbf{R}_2|} = \frac{\mathbf{R}_1 \wedge \mathbf{R}_2}{(EG - F^2)^{1/2}}$$

is the outward pointing normal. Our orthogonal unit vectors can be written as

$$\mathbf{e}_1 = \frac{\mathbf{R}_1}{E^{1/2}}, \quad \mathbf{e}_2 = \frac{\mathbf{R}_2}{G^{1/2}} \quad (1)$$

The curvature is then defined by the relation

$$\kappa_1 = \frac{L}{E}, \quad \kappa_2 = \frac{N}{G}.$$

For our curvilinear system, it is important to know how its derivatives correspond to other coordinate systems. There exists a scaling factor which arises from the mapping from one system to another. For our curvilinear coordinates, it has been shown by Myers et al. [2002] that the scaling factors m_1, m_2, m_3 are given by

$$m_1 = a_1(1 - s_3\kappa), \quad (2)$$

$$m_2 = a_2(1 - s_3\kappa), \quad (3)$$

$$m_3 = 1, \quad (4)$$

where $a_1 = E^{1/2}$ and $a_2 = G^{1/2}$. The key differential operators are shown in the appendix. We proceed to derive the thin film equations for our curvilinear coordinate system in the next section.

2 Derivation of general 3D thin film equation

Generating the thin film equations is something that has been done in many places. However, each will use their own specific nondimensionalisation and geometry. This means that when we get the final form, slight adjustments will be needed to get the form used in different papers.

2.1 Governing equation reduction

We proceed to derive the general thin film equations for an arbitrary surface using the coordinate system as introduced in the previous section. Our fluid velocity is given by $\mathbf{u} = u_1\mathbf{e}_1 + u_2\mathbf{e}_2 + u_3\mathbf{e}_3$ and has viscosity μ and density ρ . The Navier Stokes equations for an incompressible fluid are then given by:

$$\frac{\partial \mathbf{u}}{\partial t} + (\mathbf{u} \cdot \nabla) \mathbf{u} = -\frac{1}{\rho} \nabla p + \frac{\mu}{\rho} \nabla^2 \mathbf{u} + \mathbf{g} \quad (5)$$

$$\nabla \cdot \mathbf{u} = 0 \quad (6)$$

which correspond to the momentum and continuity equation respectively. These can be expressed in terms of our general coordinate system by:

$$\rho \left(\frac{\partial \mathbf{u}}{\partial t} + \sum_i \frac{u_i}{m_i} \frac{\partial \mathbf{u}}{\partial s_i} \right) = - \sum_i \left[\frac{1}{m_i} \frac{\partial p}{\partial s_i} \right] \mathbf{e}_i + \rho g \mathbf{g} + \frac{\mu}{m_1 m_2 m_3} \sum_i \frac{\partial}{\partial s_i} \left(\frac{m_j m_k}{m_i} \frac{\partial \mathbf{u}}{\partial s_i} \right), \quad (7)$$

$$\nabla \cdot \mathbf{u} = \frac{1}{m_1 m_2} \left[\frac{\partial}{\partial s_1} (m_2 u_1) + \frac{\partial}{\partial s_2} (m_1 u_2) + \frac{\partial}{\partial s_3} (m_1 m_2 u_3) \right] = 0. \quad (8)$$

We also prescribe a set of boundary conditions for our system:

- 1 The fluid satisfies a no-flux condition on the substrate,

$$u_3 = 0 \text{ on } s_3 = 0. \quad (9)$$

- 2 The fluid also has a no-slip condition on the substrate,

$$u_1 = u_2 = 0 \text{ on } s_3 = 0. \quad (10)$$

- 3 The fluids satisfies the kinematic condition on the free surface given by $s_3 = h(s_1, s_2, t)$,

$$\frac{D}{Dt} (h - z) = 0 \text{ on } s_3 = h \quad (11)$$

- 4 There is a dynamic boundary condition which relates the jump in pressure across the free surface to the curvature,

$$\Delta p = -\gamma \mathcal{K} + O(\delta) \text{ on } s_3 = h, \quad (\text{Normal}) \quad (12)$$

$$\frac{\partial u_1}{\partial s}, \frac{\partial u_2}{\partial s} = O(\delta) \text{ on } s_3 = h. \quad (\text{Tangential}) \quad (13)$$

These results for the dynamics boundary condition are based on the relationship between the cauchy stress tensor with the tangent and normal vector on the surface. Written out more fully, these conditions can be written as

$$\mathbf{n} \cdot (\sigma_{ij} n_j) = -\gamma \mathcal{K} \quad \text{on } s_3 = h, \quad (14)$$

$$\mathbf{t} \cdot (\sigma_{ij} n_j) = 0 \quad \text{on } s_3 = h. \quad (15)$$

The simplification of Equations (14) and (15) to Equations (12) and (13) are shown elsewhere in [Roy et al. \[2002\]](#).

We can rewrite the kinematic boundary condition as

$$u_3 = \frac{\partial h}{\partial t} + \frac{u_1}{m_1} \frac{\partial h}{\partial s_1} + \frac{u_2}{m_2} \frac{\partial h}{\partial s_2} \text{ on } s_3 = h(s_1, s_2, t). \quad (16)$$

Note: The condition given by Equation (13) assumes an absence of shear stress such as exists in [Myers et al. \[2002\]](#).

2.2 Non-dimensionalisation

As we want to consider the thin film problem this results in the ratio between the film height and substrate length to be quite small. The system is then nondimensionalised by the following:

$$\begin{aligned} [s_1] &= [s_2] = L, [s_3] = \delta L, \\ [\kappa_1] &= [\kappa_2] = \frac{1}{L}, \\ [u_1] &= [u_2] = U, [u_3] = \delta U, \\ [t] &= \frac{L}{U}, [p] = [p] \end{aligned}$$

where the pressure is held general for now. Under this nondimensionalisation our scaling factors now take the form:

$$m_1 = a_1 + \mathcal{O}(\delta), \quad m_2 = a_2 + \mathcal{O}(\delta), \quad m_3 = 1$$

Substituting all this into the momentum equation and taking the s_1 component yields

$$\begin{aligned} \frac{\rho U^2}{L} \left[\frac{\partial u_1}{\partial t} + \left(\frac{u_1}{a_1} + \frac{u_2}{a_2} + \delta u_3 \right) \frac{\partial u_1}{\partial s_1} \right] &= -\frac{1}{a_1} \frac{[p]}{L} \frac{\partial p}{\partial s_1} + \rho g \mathbf{g} \cdot \mathbf{e}_1 \\ &+ \frac{1}{a_1 a_2} \frac{\mu U}{L^2} \left[\frac{\partial}{\partial s_1} \left(\frac{a_2}{a_1} \frac{\partial u_1}{\partial s_1} \right) + \frac{\partial}{\partial s_2} \left(\frac{a_1}{a_2} \frac{\partial u_1}{\partial s_2} \right) + \frac{1}{\delta^2} \frac{\partial}{\partial s_3} \left(a_1 a_2 \frac{\partial u_1}{\partial s_3} \right) \right] \end{aligned} \quad (17)$$

We divide across by $\frac{\mu U}{\delta^2 L^2}$ and rearrange to give

$$\begin{aligned} \left(\frac{\delta^2 \rho [u] L}{\mu} \right) \left[\frac{\partial u_1}{\partial t} + \left(\frac{u_1}{a_1} + \frac{u_2}{a_2} + \delta u_3 \right) \frac{\partial u_1}{\partial s_1} \right] &= -\frac{1}{a_1} \frac{[p] L \delta^2}{\mu U} \frac{\partial p}{\partial s_1} + \left(\frac{\rho g (\delta L)^2}{\mu [u_1]} \right) \mathbf{g} \cdot \mathbf{e}_1 \\ &+ \frac{1}{a_1 a_2} \left[\delta^2 \frac{\partial}{\partial s_1} \left(\frac{a_2}{a_1} \frac{\partial u_1}{\partial s_1} \right) + \delta^2 \frac{\partial}{\partial s_2} \left(\frac{a_1}{a_2} \frac{\partial u_1}{\partial s_2} \right) + \frac{\partial}{\partial s_3} \left(a_1 a_2 \frac{\partial u_1}{\partial s_3} \right) \right] \end{aligned} \quad (18)$$

Finally, we define the Reynolds number by $Re = \frac{\rho [u] L}{\mu}$ and the Bond number by $B = \frac{\rho g (\delta L)^2}{\mu [u_1]}$. We also scale our pressure to match the viscous forces $[p] = \frac{\mu U}{L \delta^2}$. Thus we simplify again to

$$\begin{aligned} \delta^2 Re \left[\frac{\partial u_1}{\partial t} + \left(\frac{u_1}{a_1} + \frac{u_2}{a_2} + \delta u_3 \right) \frac{\partial u_1}{\partial s_1} \right] &= -\frac{1}{a_1} \frac{\partial p}{\partial s_1} + B \mathbf{g} \cdot \mathbf{e}_1 \\ &+ \frac{1}{a_1 a_2} \left[\delta^2 \frac{\partial}{\partial s_1} \left(\frac{a_2}{a_1} \frac{\partial u_1}{\partial s_1} \right) + \delta^2 \frac{\partial}{\partial s_2} \left(\frac{a_1}{a_2} \frac{\partial u_1}{\partial s_2} \right) + \frac{\partial}{\partial s_3} \left(a_1 a_2 \frac{\partial u_1}{\partial s_3} \right) \right] \end{aligned} \quad (19)$$

From this point we assume that $\delta^2 Re \ll 1$. In addition, we are trying to generate the thin film equations and as such the ratio of film height to substrate length should

also be small, thus $\delta \ll 1$. By taking the terms of leading order from each of the momentum equations this yields

$$\frac{1}{a_1} \frac{\partial p}{\partial s_1} = \frac{\partial^2 u_1}{\partial s_3^2} + B \mathbf{g} \cdot \mathbf{e}_1 + \mathcal{O}(\delta^2), \quad (20)$$

$$\frac{1}{a_2} \frac{\partial p}{\partial s_2} = \frac{\partial^2 u_2}{\partial s_3^2} + B \mathbf{g} \cdot \mathbf{e}_2 + \mathcal{O}(\delta^2), \quad (21)$$

$$\frac{\partial p}{\partial s_3} = \delta B \mathbf{g} \cdot \mathbf{n} + \mathcal{O}(\delta^2). \quad (22)$$

where we have retained the δB term in the leading order balance since B is undetermined.

2.3 Conservation of flux

We proceed to generate the flux equation and then integrate the reduced momentum equations to derive the thin film. Beginning with the continuity equation (8) and integrating over the film height;

$$0 = \frac{1}{a_1 a_2} \left\{ \frac{\partial}{\partial s_1} (a_2 u_1) + \frac{\partial}{\partial s_2} (a_1 u_2) + \frac{\partial}{\partial s_3} (a_1 a_2 u_3) \right\}, \quad (23)$$

$$= \int_0^h \frac{\partial}{\partial s_1} (a_2 u_1) ds_3 + \int_0^h \frac{\partial}{\partial s_2} (a_1 u_2) ds_3 + \int_0^h \frac{\partial}{\partial s_3} (a_1 a_2 u_3) ds_3, \quad (24)$$

$$= \int_0^h \frac{\partial}{\partial s_1} (a_2 u_1) ds_3 + \int_0^h \frac{\partial}{\partial s_2} (a_1 u_2) ds_3 + [a_1 a_2 u_3]_0^h, \quad (25)$$

$$= \int_0^h \frac{\partial}{\partial s_1} (a_2 u_1) ds_3 + \int_0^h \frac{\partial}{\partial s_2} (a_1 u_2) ds_3 + a_1 a_2 \left(\frac{\partial h}{\partial t} + \frac{u_1}{a_1} \frac{\partial h}{\partial s_1} + \frac{u_2}{a_2} \frac{\partial h}{\partial s_2} \right), \quad (26)$$

$$= \frac{\partial}{\partial s_1} \int_0^h a_2 u_1 ds_3 + \frac{\partial}{\partial s_2} \int_0^h a_1 u_2 ds_3 + a_1 a_2 \frac{\partial h}{\partial t} \quad (27)$$

In Equation (26) we used the kinematic boundary condition on the free surface as well as the no flux on the substrate. Our final conservation of flux equation is given by

$$a_1 a_2 \frac{\partial h}{\partial t} + \frac{\partial Q_1}{\partial s_1} + \frac{\partial Q_2}{\partial s_2} = 0 \text{ on } s_3 = h, \quad (28)$$

where

$$Q_1 = \int_0^h a_2 u_1 ds_3, \quad (29)$$

$$Q_2 = \int_0^h a_1 u_2 ds_3. \quad (30)$$

2.4 Thin film PDE

Starting with the last of our momentum equation we proceed to solve for the pressure. Under our nondimensionalisation Equation (12) becomes

$$\Delta p = -\mathcal{C}\mathcal{K} \text{ on } s_3 = h, \quad (31)$$

where $\mathcal{C} = \frac{\gamma\delta^2}{\mu U}$ is the capillary number. Then, integrating Equation (22) gives

$$p(s_3) - p(h) = \Delta p = C_1 + \delta B(\mathbf{g} \cdot \mathbf{n})(s_3 - h) + \mathcal{O}(\delta^2, \delta^3 Re) \quad (32)$$

where C_1 is a function of s_1, s_2, t . Applying the dynamic boundary condition gives that $C_1 = -\mathcal{C}\mathcal{K}$. In this case, we have taken atmospheric pressure to be zero. Thus the pressure jump is simply given by the internal pressure and so

$$p = -\mathcal{C}\mathcal{K} + \delta B(\mathbf{g} \cdot \mathbf{n})(s_3 - h) + \mathcal{O}(\delta^2, \delta^3 Re). \quad (33)$$

Taking the s_i derivative of the pressure for $i = 1, 2$ gives

$$\frac{\partial p}{\partial s_i} = -\mathcal{C} \frac{\partial \mathcal{K}}{\partial s_i} + \delta B(\mathbf{g} \cdot \mathbf{n}) \frac{\partial h}{\partial s_i},$$

which is independent of s_3 . Hence we can easily integrate Equations (20) and (21) to find the speed. We do this for u_1 noting that the process is the same for u_2 . Integrating twice and applying the tangential dynamic boundary condition and the no-slip condition gives us

$$u_1 = \left(\frac{1}{a_1} \frac{\partial p}{\partial s_1} - B\mathbf{g} \cdot \mathbf{e}_1 \right) \left(\frac{s_3^2}{2} - hs_3 \right), \quad (34)$$

This allows us to calculate the fluxes.

$$\begin{aligned} Q_1 &= \int_0^h a_2 u_1 ds_3, \\ &= a_2 \left(\frac{1}{a_1} \frac{\partial p}{\partial s_1} - B\mathbf{g} \cdot \mathbf{e}_1 \right) \left[\frac{s_3^6}{2} - \frac{hs_3^2}{2} \right]_0^h, \\ &= -a_2 \left(\frac{1}{a_1} \frac{\partial p}{\partial s_1} - B\mathbf{g} \cdot \mathbf{e}_1 \right) \frac{h^3}{3}, \\ \Rightarrow Q_2 &= -a_1 \left(\frac{1}{a_2} \frac{\partial p}{\partial s_2} - B\mathbf{g} \cdot \mathbf{e}_2 \right) \frac{h^3}{3} \end{aligned} \quad (35)$$

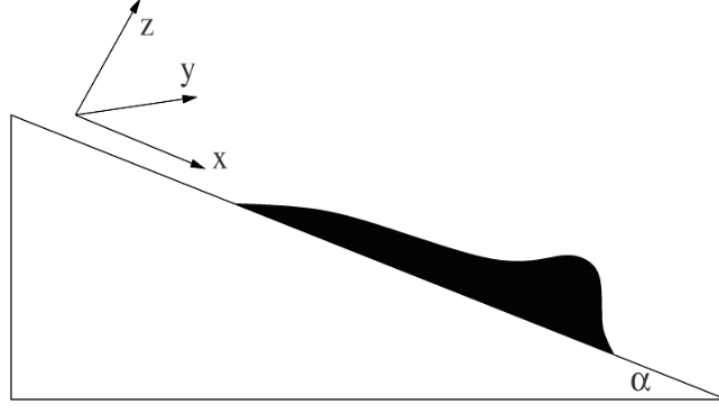


Figure 2: Sketch of the two-dimensional fluid geometry as from [Kondic \[2003\]](#)

We then substitute our fluxes into our conservation of flux equation (28):

$$\begin{aligned}
0 &= \frac{\partial h}{\partial t} + \frac{1}{a_1 a_2} \left\{ \frac{\partial Q_1}{\partial s_1} + \frac{\partial Q_2}{\partial s_2} \right\}, \\
&= \frac{\partial h}{\partial t} - \frac{1}{a_1 a_2} \left(\frac{\partial}{\partial s_1} a_2 \left(\frac{1}{a_1} \frac{\partial p}{\partial s_1} - B \mathbf{g} \cdot \mathbf{e}_1 \right) \frac{h^3}{3} - \frac{\partial}{\partial s_2} a_1 \left(\frac{1}{a_2} \frac{\partial p}{\partial s_2} - B \mathbf{g} \cdot \mathbf{e}_2 \right) \frac{h^3}{3} \right), \\
&= \frac{\partial h}{\partial t} - \frac{1}{a_1 a_2} \left(a_2 \frac{\partial}{\partial s_1} \left(\frac{1}{a_1} \frac{\partial p}{\partial s_1} - B \mathbf{g} \cdot \mathbf{e}_1 \right) \frac{h^3}{3} - a_1 \frac{\partial}{\partial s_2} \left(\frac{1}{a_2} \frac{\partial p}{\partial s_2} - B \mathbf{g} \cdot \mathbf{e}_2 \right) \frac{h^3}{3} \right), \\
&= \frac{\partial h}{\partial t} - \nabla_s \cdot \left\{ \left(\frac{1}{a_1} \frac{\partial p}{\partial s_1} - B \mathbf{g} \cdot \mathbf{e}_1 \right) \frac{h^3}{3} \mathbf{e}_1 + \left(\frac{1}{a_2} \frac{\partial p}{\partial s_2} - B \mathbf{g} \cdot \mathbf{e}_2 \right) \frac{h^3}{3} \mathbf{e}_2 \right\}, \\
&= \frac{\partial h}{\partial t} - \nabla_s \cdot \left\{ \frac{h^3}{3} \left[\nabla_s p - \sum_{i=1}^2 B(\mathbf{g} \cdot \mathbf{e}_i) \mathbf{e}_i \right] \right\}
\end{aligned} \tag{36}$$

Finally, we plug in our value obtained for pressure in Equation (33) to get the final thin film equation:

$$\frac{\partial h}{\partial t} + \nabla_s \cdot \left\{ \frac{h^3}{3} \left[C \nabla_s \mathcal{K} + \delta B(\mathbf{g} \cdot \mathbf{n}) \nabla_s h + \sum_{i=1}^2 B(\mathbf{g} \cdot \mathbf{e}_i) \mathbf{e}_i \right] \right\} = 0. \tag{37}$$

2.5 Examples of substrates

2.5.1 Flat incline

Working with the geometry as shown in Figure 2, this results in a simple coordinate system where we can define $s_1 = x$, $s_2 = y$, $s_3 = z$ and the scaling factors $m_1 = m_2 = m_3 = 1$. Under this geometry the surface divergence operator becomes the normal divergence operator and similarly with the surface gradient. Since this is a planar

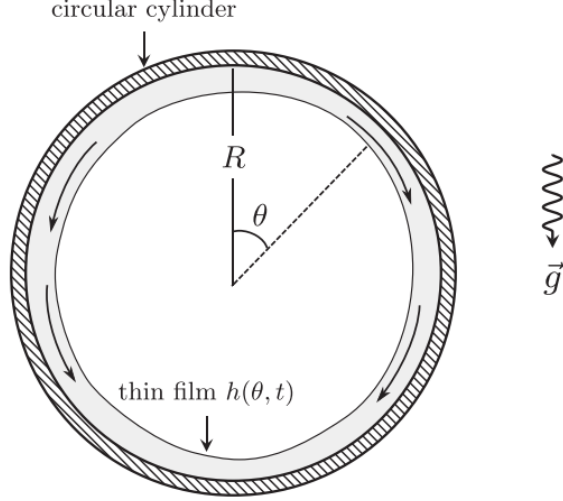


Figure 3: Geometry of the circular cylinder with gravity acting down and the $z = s_3$ component going into the page. Figure from [Trinh et al. \[2014\]](#).

surface, the curvature will be zero. Beginning with Equation (37) we have

$$\begin{aligned}
\frac{\partial h}{\partial t} + \nabla_s \cdot \left\{ \frac{h^3}{3} \left[\mathcal{C} \nabla_s \mathcal{K} + \delta B (\mathbf{g} \cdot \mathbf{n}) \nabla_s h + \sum_{i=1}^2 B (\mathbf{g} \cdot \mathbf{e}_i) \mathbf{e}_i \right] \right\} &= 0, \\
\frac{\partial h}{\partial t} + \nabla \cdot \left\{ \frac{h^3}{3} \left[\mathcal{C} \nabla (\delta \nabla^2 h) + \delta B (\mathbf{g} \cdot \mathbf{n}) \nabla h + \sum_{i=1}^2 B (\mathbf{g} \cdot \mathbf{e}_i) \mathbf{e}_i \right] \right\} &= 0, \quad (38) \\
\frac{\partial h}{\partial t} + \nabla \cdot \left\{ \frac{h^3}{3} [\delta \mathcal{C} \nabla \nabla^2 h - \delta B \cos \theta \nabla h + B \sin \theta \mathbf{e}_1] \right\} &= 0,
\end{aligned}$$

2.5.2 Cylinder

We take the case of a cylinder of radius R as in Figure 3. Our parametrisation is then given by $s_1 = R\theta$, $s_2 = z$ as in [Myers et al. \[2002\]](#). The substrate is then defined by $\mathbf{R} = (R \cos \theta, R \sin \theta, 0)$ and the normal for flow on the inside and outside of the cylinder are given by $\mp(\cos \theta, \sin \theta, 0)$ respectively. This then allows calculation of the fundamental forms. Calculating E is given by

$$\begin{aligned}
E &= \frac{\partial \mathbf{R}}{\partial s_1} \cdot \frac{\partial \mathbf{R}}{\partial s_1}, \\
&= [\mp(-\sin \theta, \cos \theta, 0)] \cdot [\mp(-\sin \theta, \cos \theta, 0)], \\
&= 1.
\end{aligned} \quad (39)$$

From following the same procedure, we find that $G = 1, L = \pm \frac{1}{R}, N = 0$ and that the curvatures are given by $\kappa_1 = \pm \frac{1}{R}, \kappa_2 = 0$. Under this choice of s_1, s_2 , the scaling factors are all equal to one. This results in the surface operators being equivalent to the normal operators. Beginning with our thin film equation (37)

$$\begin{aligned}
\frac{\partial h}{\partial t} + \nabla_s \cdot \left\{ \frac{h^3}{3} \left[\mathcal{C} \nabla_s \mathcal{K} + \delta B (\mathbf{g} \cdot \mathbf{n}) \nabla_s h + \sum_{i=1}^2 B (\mathbf{g} \cdot \mathbf{e}_i) \mathbf{e}_i \right] \right\} &= 0, \\
\frac{\partial h}{\partial t} + \nabla \cdot \left\{ \frac{h^3}{3} \left[\mathcal{C} \nabla (\kappa_1 + \delta h \kappa_1^2 + \delta \nabla^2 h) + \delta B (\mathbf{g} \cdot \mathbf{n}) \nabla h + \sum_{i=1}^2 B (\mathbf{g} \cdot \mathbf{e}_i) \mathbf{e}_i \right] \right\} &= 0, \\
\frac{\partial h}{\partial t} + \nabla \cdot \left\{ \frac{h^3}{3} \left[\mathcal{C} \frac{1}{R} \frac{\partial}{\partial \theta} (\delta h \kappa_1^2 + \delta \nabla^2 h) \mathbf{e}_1 + \mathcal{C} \frac{\partial}{\partial z} (\delta h \kappa_1^2 + \delta \nabla^2 h) \mathbf{e}_2 + \right. \right. \\
\left. \left. \delta B (\mathbf{g} \cdot \mathbf{n}) \frac{1}{R} \frac{\partial h}{\partial \theta} \mathbf{e}_1 + \delta B (\mathbf{g} \cdot \mathbf{n}) \frac{\partial h}{\partial z} \mathbf{e}_2 + \sum_{i=1}^2 B (\mathbf{g} \cdot \mathbf{e}_i) \mathbf{e}_i \right] \right\} &= 0, \\
\frac{\partial h}{\partial t} + \frac{1}{R} \frac{\partial}{\partial \theta} \left\{ \frac{h^3}{3} \left(\delta \left[\mathcal{C} \frac{1}{R} \frac{\partial}{\partial \theta} \left(\frac{h}{R^2} + \nabla^2 h \right) + B (\mathbf{g} \cdot \mathbf{n}) \frac{1}{R} \frac{\partial h}{\partial \theta} \right] + B (\mathbf{g} \cdot \mathbf{e}_1) \right) \right\} \\
+ \frac{\partial}{\partial z} \left\{ \frac{h^3}{3} \left(\delta \left[\mathcal{C} \frac{\partial}{\partial z} \left(\frac{h}{R^2} + \nabla^2 h \right) + B (\mathbf{g} \cdot \mathbf{n}) \frac{\partial h}{\partial z} \right] + B (\mathbf{g} \cdot \mathbf{e}_2) \right) \right\} &= 0
\end{aligned} \tag{40}$$

In the case where the cylinder is of unit length and gravity is of the form $\mathbf{g} = -\cos\theta \mathbf{n} + \sin\theta \mathbf{e}_1$, this is similar to the form as given in King et al. [2007] for their case of $\alpha = 0$,

$$\begin{aligned}
\frac{\partial h}{\partial t} + \frac{\partial}{\partial \theta} \left\{ \frac{h^3}{3} \left(\delta \left[\mathcal{C} \frac{\partial}{\partial \theta} (h + \nabla^2 h) + B \cos\theta \frac{\partial h}{\partial \theta} \right] + B \sin\theta \right) \right\} \\
+ \frac{\partial}{\partial z} \left\{ \frac{\delta h^3}{3} \left[\mathcal{C} \frac{\partial}{\partial z} (h + \nabla^2 h) + B \cos\theta \frac{\partial h}{\partial z} \right] \right\} &= 0,
\end{aligned} \tag{41}$$

where we have an extra term in the form of $\delta B \cos\theta$ which corresponds to the normal component of gravity.

In the case that our film height is independent of $s_3 = z$, then this simplifies to the form

$$\frac{\partial h}{\partial t} + \frac{\partial}{\partial \theta} \left\{ \frac{h^3}{3} [\delta \mathcal{C} (h_\theta + h_{\theta\theta\theta}) + \delta B \cos\theta_\theta] + B \sin\theta \right\} = 0. \tag{42}$$

3 Kondic & Lin

3.1 Thin films flowing down inverted substrate

3.1.1 Formulation

In the paper published by [Lin and Kondic \[2010\]](#), they examined the stability of thin films on an inverted substrate. Under their nondimensionalisation, they established a key parameter D by which variations led to wave like behaviour forming.

To reduce our problem to their formulation, we start with our example for an incline plane given by

$$\frac{\partial h}{\partial t} + \nabla \cdot \left\{ \frac{h^3}{3} [\delta \mathcal{C} \nabla \nabla^2 h - \delta B \cos \theta \nabla h + B \sin \theta \mathbf{e}_1] \right\} = 0 \quad (43)$$

They have rescaled their velocity by $U = \frac{\rho g h_0^2 \sin \alpha}{3\mu}$. This is equivalent to setting $\frac{B \sin \theta}{3} = 1$ for our incline formulation. From our second term in the brackets this results in $\delta \rightarrow (3Ca)^{1/3}$ relation. Finally, examining the first term in the brackets, based on our nondimensionalisation:

$$\begin{aligned} \frac{\delta \mathcal{C}}{3} &= \frac{\delta^3 \gamma}{3\mu U}, \\ &= \frac{3Ca\gamma}{3\mu U}, \\ &= 1, \end{aligned} \quad (44)$$

since they have defined their Capillary number as $Ca = \frac{\mu U}{\gamma}$.

Thus, their governing equation is given by

$$\frac{\partial h}{\partial t} + \nabla \cdot [h^3 \nabla \nabla^2 h] - D \nabla \cdot [h^3 \nabla h] + \frac{\partial h^3}{\partial x} = 0 \quad (45)$$

where $D = (3Ca)^{1/3} \cot \alpha$ and measures the normal component of gravity.

They proceed to examine the 2D setting where $h = h(x, t)$ where h is y -independent. Under this simplification the master equation is given as

$$\frac{\partial h}{\partial t} + [h^3 (h_{xxx} - Dh_x + 1)]_x = 0. \quad (46)$$

The boundary conditions are chosen so that the height is always 1 at $x = 0$ and there is a constant flux.

$$h(0, t) = 0, \quad (47)$$

$$h_{xxx}(0, t) - Dh_x(0, t) = 0. \quad (48)$$

In addition, they have added a small layer of wetness along the entire plane. This precursor is given a thickness b . For a substrate of length L , this adds the other two boundary conditions:

$$h(L, t) = b, \quad (49)$$

$$h_x(L, t) = 0. \quad (50)$$

3.1.2 Results

Under this model, variation in the D parameter allowed observation of wave behaviour in the system. This was studied for negative values of D which correspond to an inverted substrate. Different regimes were found for decreasing values of D .

- Type 1 For $-1.1 \leq D < 0$ a strong capillary ridge forms behind the wave front. An additional heavily damped oscillation can be seen behind as shown in Figure 4a. The wave speed reach a value constant to $U = 1 + b + b^2$. Analysis on this type will be discussed in the next section.
- Type 2 For $-1.9 \leq D < 1.1$, a wave train follows behind the capillary ridge. These waves move faster than the front itself. Three different states are found behind the ridge, two types of waves and a constant state as in Figure 4b.
- Type 3 Finally, the regime $-3 \leq D < 1.9$ is a holds nonlinear steady travelling waves. The nature of these changes as the magnitude of D increases with solitary waves for large magnitude (Figure 4d) and more sinusoidal for lower magnitude (Figure 4c).

3.1.3 Analysis

Travelling Wave In the regime of type 1, we expect a wave front which reaches a constant speed. Thus we assume a travelling wave for our system and rewrite $H(s) = h(x, t)$ where we have set $s = x - Ut$. Plugging into Equation (46) gives

$$\begin{aligned} \frac{\partial H}{\partial s} \frac{\partial s}{\partial t} + \frac{\partial}{\partial s} [H^3(H_{sss} - DH_s + 1)] &= 0, \\ -U \frac{\partial H}{\partial s} + \frac{\partial}{\partial s} [H^3(H_{sss} - DH_s + 1)] &= 0, \\ -UH + [H^3(H_{sss} - DH_s + 1)] &= c. \end{aligned} \tag{51}$$

Imposing the condition that $H \rightarrow 1$ as $s \rightarrow -\infty$ gives

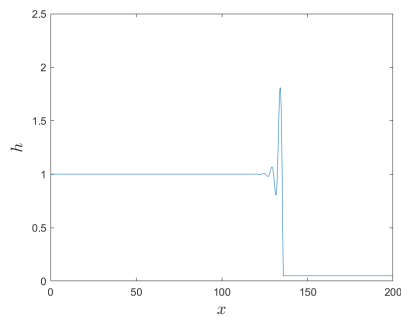
$$-U + 1 = c. \tag{52}$$

Then imposing the other boundary condition of $H \rightarrow b$ as $s \rightarrow \infty$ gives

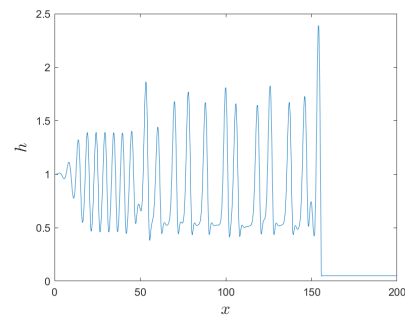
$$-Ub + b^3 = c. \tag{53}$$

Solving for U and c gives us that $U = 1 + b + b^2$ and $c = -b - b^2$.

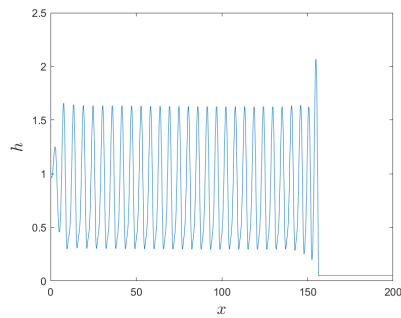
Linear Stability Analysis For the type 1 regime, we want to observe what happens under a small perturbation. We use linear stability analysis and assume that the height of the thin film away from the capillary ridge is given by $h(x, t) = 1 + \xi(x, t)$ where $\xi \ll 1$. We plug this into Equation (46) and look for terms of the first order:



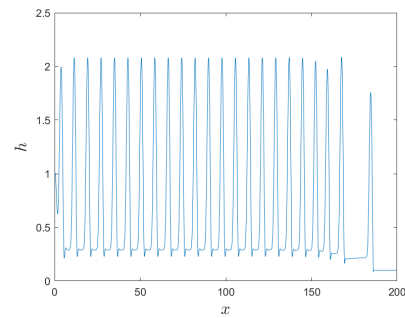
(a) Final profile of thin film for $D = -1.0$ at $t = 400$.



(b) Wave profile of thin film down an inverted substrate for $D = -1.5$ at $t = 400$.



(c) Wave profile for $D = -2.0$ at $t = 400$.



(d) Profile for $D = -2.5$ at $t = 350$.

Figure 4: Profile of thin film evolution for time snapshot at $t = 400$ for (a-c) and $t = 350$ for (d) for various values of D .

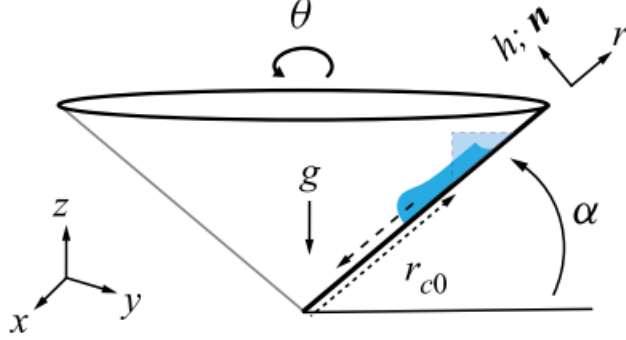


Figure 5: Geometry of the funnel as in Lin et al. [2021].

$$\begin{aligned}
\frac{\partial \xi}{\partial t} + [(1 + \xi)^3 (\xi_{xxx} - D\xi_x + 1)]_x &= 0, \\
\frac{\partial \xi}{\partial t} + [(1 + 3\xi + 3\xi^2 + \xi^3) (\xi_{xxx} - D\xi_x + 1)]_x &= 0, \\
\frac{\partial \xi}{\partial t} + [\xi_{xxx} - D\xi_x + 3\xi]_x + \mathcal{O}(\xi^2) &= 0, \\
\xi_t + \xi_{xxxx} - D\xi_{xx} + 3\xi_x &= 0.
\end{aligned} \tag{54}$$

We let $\xi \sim \exp i(kx - \omega t)$ where $\omega = \omega_r + i\omega_i$ and plug this in to obtain the dispersion relation

$$-i(\omega_r + i\omega_i) + k^4 + Dk^2 + 3ik = 0, \tag{55}$$

which gives the following relations

$$\omega_r = 3k, \tag{56}$$

$$\omega_i = -(k^4 + Dk^2). \tag{57}$$

We are concerned with the ω_i term as it turns out to be the real component of ξ . Thus for $\omega_i < 0$, the real component is negative and any perturbations will die out. However, for $D < 0$ it reaches a critical point where the critical wave number is given by $k_c = \sqrt{-D}$. In addition, by looking at the first relation, we get that the linear waves has a speed of 3 which is larger than the travelling wave speed U as discussed in the previous section.

3.2 Thin liquid films in a funnel

Following on from the inverted substrated Lin et al. [2021] continued on to examine a funnel. The problem's geometry is shown in Figure 5 where we see the principal directions given by $s_1 = r$ and $s_2 = \theta$. The funnel has opening angle α and is parameterised by

$$\mathbf{R} = (r \cos \alpha \cos \theta, r \cos \alpha \sin \theta, r \sin \alpha), \quad r \in [R_l, R_r], \quad \theta \in [0, 2\pi]. \tag{58}$$

We note that r is contained in an interval where R_l is far away from the nose of the cone to avoid the singularity. Calculating our fundamental forms we find that

$$\begin{aligned} E &= 1, & G &= r^2 \cos^2 \alpha, \\ L &= 0, & N &= r \cos \alpha \sin \alpha \end{aligned}$$

and from Equation (1) we find out unit vectors and normal on the funnel to be

$$\mathbf{e}_1 = (\cos \alpha \cos \theta, \cos \alpha \sin \theta, \sin \alpha), \quad (59)$$

$$\mathbf{e}_2 = (-\sin \theta, \cos \theta, 0), \quad (60)$$

$$\mathbf{n} = (-\sin \alpha \cos \theta, -\sin \alpha \sin \theta, \cos \alpha). \quad (61)$$

From our fundamental forms we find the curvatures to be $\kappa_1 = 0$ and $\kappa_2 = \frac{\tan \alpha}{r}$. In this setting, the gravitational component can be written as $\mathbf{g} = (0, 0, -1)$ and thus we can rewrite our thin film equation (37) as

$$\frac{\partial h}{\partial t} + \nabla_s \cdot \left\{ \frac{h^3}{3} [\mathcal{C} \nabla_s \mathcal{K} - \delta B \cos \alpha \nabla_s h - B \sin \alpha \mathbf{e}_1] \right\} = 0. \quad (62)$$

Replacing for the curvature and an adjustment to the nondimensionalisation gives their form of

$$\frac{\partial h}{\partial t} + \nabla_s \cdot \left\{ h^3 \left[\nabla_s \left(\nabla_s^2 h + \frac{\tan \alpha}{r} \right) - \cos \alpha \nabla_s h - \sin \alpha \mathbf{e}_1 \right] \right\} = 0. \quad (63)$$

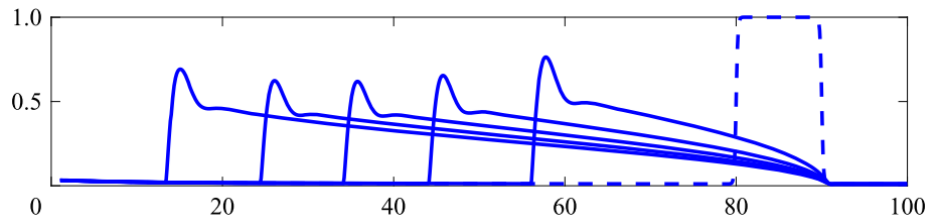
From this point on, they consider three steps.

- 1 *Self similar*: They initially examine the system in the absence of surface tension keeping only the substrate curvature and tangential gravity components. Assuming a solution of the form

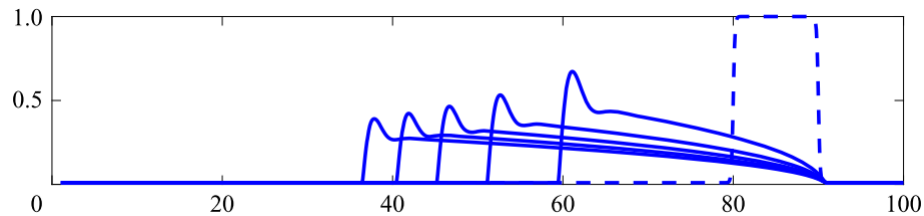
$$h(r, t) = T(t)H(\eta), \quad \eta = \frac{R - r}{r_f(t)}, \quad (64)$$

- where R is the position on the hill where the fluid was initial deposited $r_f(t)$ is the position travelled by the front and $R - r_f(t)$ is the position of the front - for small times they find the film height at the front to be $h(r = R - r_f(t), t) = \left(\frac{\tilde{v}_c}{2c_s} \right)^{1/3} t^{-1/3}$. Here \tilde{v}_c is found via a column constraint and $c_s = \sin \alpha + \tan \alpha / R^2$. Thus, when the fluid flows only a short distance down the funnel, this is identical to flow down a plane as found in Kondic [2003]. However, for flow down a funnel, while initially the film height will decrease, as the fluid converges to the center, it will begin to increase again.

- 2 *Constant volume, convergence*: In order to gain insight in the nature of the funnel flow as the fluid converges, they take the self similar solution and impose a fixed volume constraint. The result that they find is that the front begins to accelerate as it approaches the funnel center. Looking at Figures 6a and 6b which compares the difference between the funnel and the plane, we see in Figure 6a the increasing film height as the front moves closer to the center.



(a) Height profile of thin film down a funnel.



(b) Wave profile of thin film down an inverted substrate.

Figure 6: Constant volume flow for a (a) funnel (b) inverted plane. Taken from Lin et al. [2021].

3 *Instability*: The stability analysis for the funnel becomes a lot more complex than the incline plane especially for constant volume. The base consideration is the constant flux problem where the thickness of the film doesn't depend on the transverse coordinate. In this case, the fluid moves down the slope with a constant speed U which results in them taking a move frame in which the base state is time independent. For this problem of flow in a funnel, the convergent nature of the film means that the base state is evolving. Ultimately, they take a rather simplistic approach, where they take a snapshot in time taking key quantities such as the opening angle α , and a thickness h_0 which is the film thickness behind the capillary ridge. Using these, they then match this to a solution from the incline plane which has the same characteristics, thus generating the critical wavenumbers.

4 Final remarks

4.1 Huppert & Takagi

Takagi and Huppert [2010] conducted a series of experiments to observe how a fluid such as glycerine or golden syrup would evolve on the top side of a cylinder or sphere driven by gravity. In these experiments a fixed volume of fluid was placed on top. A series of snapshots from the spherical ball case are shown in Figures 7a, 7b and 7c. Accompanying the experiments was a series of analysis for thickness of the flow. For

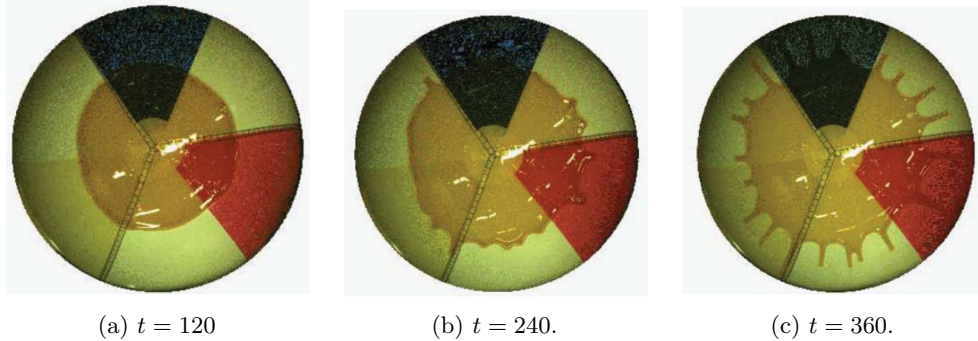


Figure 7: Snapshots of the flow of golden syrup down a beachball. In (b) we observe instabilities forming in the front which leads to rivulets forming in (c). Taken from [Takagi and Huppert \[2010\]](#).

the cylindrical case their dimensional governing equation was

$$\frac{\partial h}{\partial t} + \frac{g}{3\mu R} \frac{\partial}{\partial \theta} (\sin \theta h^3) = 0. \quad (65)$$

By scaling with regards to the cross sectional area, for small θ they found the height of the film to be of the form:

$$h(t) = \left(\frac{3R\mu}{2g} \right)^{1/2} t^{-1/2} \quad (66)$$

and thus independent of θ as well as decreasing like $t^{-1/2}$. However, this only holds for small θ and before instabilities results in the front splitting to rivulets. Performing a similar analysis in the case of the sphere, they again find a similar result for the evolution of the film height which agrees with experiment under the same conditions as the cylinder. Experimentally it was shown that these rivulets do not develop in the case of large initial volume.

4.2 Open Challenges

Through this reading course there has been two fundamental objectives: (i) to get more familiar with differential geometry on curved surfaces (ii) to understand what different research groups have done concerning stability analysis on these (complex) surfaces. With regards to stability analysis on these complex surfaces, very little has actually been done, where from the case of Lin & Kondic initial analysis was done on a plane, and then analysis from the funnel was mapped to the results of the plane. Thus, one of the obvious open challenges is can the linear stability analysis be applied to geometries such as a cylinder and sphere - and if it agrees with experimental work - and if so, to other more complex surfaces. Regarding the cylinder and sphere, while these have constant curvature, as the fluid drips down the different components of gravity will change providing a clear distinction from the planar case. Are their

regimes on top of a cylinder or sphere where this doesn't play an important role? Certainly the question of whether we can measure the wavenumbers under which instabilities form and what adaptations of the method used by Lin & Kondic is of great interest.

4.3 Conclusion

Over the course of this report we have derived the three-dimensional thin film equation for an arbitrary surface using curvilinear coordinates. From this we provided examples of how this simplifies to classical geometries such as a plane and cylinder. Using these examples we studied how thin film instabilities form on an inverted plane using linear stability analysis. We then proceeded to summarise the paper by Lin et al. [2021] on thin films down a funnel. Finally we have briefly accounted for the results by Takagi and Huppert [2010] on syrup down a beach ball and raised the main open challenges that has arisen through this reading course.

5 Appendix

$$\begin{aligned}
\nabla &= \sum_i \frac{e_i}{m_i} \frac{\partial}{\partial q_i} \\
\nabla \cdot \mathbf{u} &= \frac{1}{m_1 m_2 m_3} \left[\frac{\partial}{\partial q_1} (m_2 m_3 u_1) + \frac{\partial}{\partial q_2} (m_1 m_3 u_2) + \frac{\partial}{\partial q_3} (m_1 m_2 u_3) \right] \\
&= \frac{1}{m_1 m_2 m_3} \sum_{i=0}^3 \frac{\partial}{\partial q_i} (m_j m_k u_i) \\
\nabla^2 &= \frac{1}{m_1 m_2 m_3} \left[\frac{\partial}{\partial q_1} \left(\frac{m_2 m_3}{m_1} \frac{\partial}{\partial q_1} \right) + \frac{\partial}{\partial q_2} \left(\frac{m_3 m_1}{m_2} \frac{\partial}{\partial q_2} \right) + \frac{\partial}{\partial q_3} \left(\frac{m_1 m_2}{m_3} \frac{\partial}{\partial q_3} \right) \right] \\
&= \frac{1}{m_1 m_2 m_3} \sum_{i=0}^3 \frac{\partial}{\partial q_i} \left(\frac{m_j m_k}{m_i} \frac{\partial}{\partial q_i} \right)
\end{aligned} \tag{67}$$

5.1 Surface Operations

$$\begin{aligned}
\nabla_s \cdot (q_1 \mathbf{e}_1 + q_2 \mathbf{e}_2) &= \frac{1}{a_1 a_2} \left[\frac{\partial}{\partial x_1} (a_2 q_1) + \frac{\partial}{\partial x_2} (a_1 q_2) \right] \\
\nabla_s &= \frac{\partial}{\partial x_1} \frac{\mathbf{e}_1}{a_1} + \frac{\partial}{\partial x_2} \frac{\mathbf{e}_2}{a_2} \\
\nabla_s^2 &= \frac{1}{a_1 a_2} \left[\frac{\partial}{\partial x_1} \left(\frac{a_2}{a_1} \frac{\partial}{\partial x_1} \right) + \frac{\partial}{\partial x_2} \left(\frac{a_1}{a_2} \frac{\partial}{\partial x_2} \right) \right]
\end{aligned} \tag{68}$$

References

- Gioele Balestra, David Minh-Phuc Nguyen, and François Gallaire. Rayleigh-taylor instability under a spherical substrate. *Physical Review Fluids*, 3(8):084005, 2018.
- PD Howell. Surface-tension-driven flow on a moving curved surface. *Journal of engineering mathematics*, 45(3):283–308, 2003.
- AC King, EO Tuck, and J-M Vanden-Broeck. Air-blown waves on thin viscous sheets. *Physics of Fluids A: Fluid Dynamics*, 5(4):973–978, 1993.
- Andrew A King, Linda J Cummings, Shailesh Naire, and Oliver E Jensen. Liquid film dynamics in horizontal and tilted tubes: Dry spots and sliding drops. *Physics of Fluids*, 19(4):042102, 2007.
- Lou Kondic. Instabilities in gravity driven flow of thin fluid films. *Siam review*, 45(1):95–115, 2003.
- T-S Lin, L Kondic, and A Filippov. Thin films flowing down inverted substrates: Three-dimensional flow. *Physics of Fluids*, 24(2):022105, 2012.
- T-S Lin, JA Dijkstra, and L Kondic. Thin liquid films in a funnel. *Journal of Fluid Mechanics*, 924, 2021.
- Te-Sheng Lin and Lou Kondic. Thin films flowing down inverted substrates: Two dimensional flow. *Physics of Fluids*, 22(5):052105, 2010.
- JA Moriarty, LW Schwartz, and EO Tuck. Unsteady spreading of thin liquid films with small surface tension. *Physics of Fluids A: Fluid Dynamics*, 3(5):733–742, 1991.
- Tim G Myers. Thin films with high surface tension. *SIAM review*, 40(3):441–462, 1998.
- Tim G Myers, Jean PF Charpin, and S Jon Chapman. The flow and solidification of a thin fluid film on an arbitrary three-dimensional surface. *Physics of Fluids*, 14(8):2788–2803, 2002.
- R Valery Roy, AJ Roberts, and ME Simpson. A lubrication model of coating flows over a curved substrate in space. *Journal of Fluid Mechanics*, 454:235–261, 2002.
- LW Schwartz and DE Weidner. Modeling of coating flows on curved surfaces. *Journal of engineering mathematics*, 29(1):91–103, 1995.
- Daisuke Takagi and Herbert E Huppert. Flow and instability of thin films on a cylinder and sphere. *Journal of Fluid Mechanics*, 647:221–238, 2010.
- Philippe H Trinh, Hyungsoo Kim, Naima Hammoud, Peter D Howell, S Jonathan Chapman, and Howard A Stone. Curvature suppresses the rayleigh-taylor instability. *Physics of Fluids*, 26(5):051704, 2014.
- CY Wang. Thin film flowing down a curved surface. *Zeitschrift für angewandte Mathematik und Physik ZAMP*, 35(4):532–544, 1984.